ACS APPLIED MATERIALS & INTERFACES

Article

Photoelectrochemical DNA Biosensor Based on Dual Signal Amplification Strategy Integrating Inorganic-Organic Nanocomposites Sensitization with #-Exonuclease Assisted Target Recycling

Xiao-Mei Shi, Gao-Chao Fan, Qingming Shen, and Jun-Jie Zhu

ACS Appl. Mater. Interfaces, **Just Accepted Manuscript** • DOI: 10.1021/acsami.6b14466 • Publication Date (Web): 08 Dec 2016

ACS Publications

ACS Applied Materials & Interfaces is published by the American Chemical Society.
1155 Sixteenth Street N.W., Washington, DC 20036

Photoelectrochemical DNA Biosensor Based on Dual Signal Amplification Strategy Integrating Inorganic-Organic Nanocomposites Sensitization with λ-Exonuclease Assisted Target Recycling

Xiao-Mei Shi,[†,‡,1] Gao-Chao Fan,[‡,1] Qingming Shen,[†,] and Jun-Jie Zhu [‡,*]*

[†] Key Laboratory for Organic Electronics and Information Displays & Institute of Advanced Materials, Jiangsu National Synergetic Innovation Center for Advanced Materials (SICAM), Nanjing University of Posts & Telecommunications, Nanjing, 210023, P. R. China

[‡] State Key Laboratory of Analytical Chemistry for Life Science, School of Chemistry and Chemical Engineering, Nanjing University, Nanjing, 210093, P. R. China

Abstract: Sensitive and accurate analysis of DNA is crucial to better understanding of DNA functions and early diagnosis of fatal disease. Herein, an enhanced photoelectrochemical (PEC) DNA biosensor was proposed based on dual signal amplification via coupling inorganic-organic nanocomposites sensitization with λ-exonuclease (λ-Exo) assisted target recycling. The short DNA sequence about Chronic Myelogenous Leukemia (CML, Type b3a2) was selected as target DNA (tDNA). ZnO nanoplates were deposited with CdS nanocrystals to form ZnO/CdS hetero-nanostructure and it was used as PEC substrate for immobilizing hairpin DNA (hDNA). CdTe quantum dots (QDs) covalently linked with meso-tetra(4-carboxyphenyl)porphine (TCPP) to form CdTe/TCPP inorganic-organic nanocomposites, which were utilized as sensitization agents

labeling at the terminal of probe DNA (pDNA). When the hDNA modified sensing electrode was incubated with tDNA and λ-Exo, hDNA hybridized with tDNA and meanwhile it could be recognized and cleaved by λ-Exo, resulting in the release of tDNA. The rest of non-hybridized hDNA would continuously hybridize with the released tDNA, cleave by λ-Exo, and set free the tDNA again. After λ-Exo assisted tDNA recycling, more amounts of short DNA (sDNA) fragments coming from digestion of hDNA produced on the electrode and hybridized with CdTe/TCPP labeled pDNA (pDNA-CdTe/TCPP conjugates). In this case, the sensitization of CdTe/TCPP inorganic-organic nanocomposites occurred, which evidently extend the absorption range and strengthened the absorption intensity of light energy, and accordingly the photocurrent signal significantly promoted. Through introducing the dual signal amplification tactics, the developed PEC assay allowed a low calculated detection limit of 25.6 aM with a wide detection scope from 0.1 fM to 5 pM for sensitive and selective determination of tDNA.

Keywords: photoelectrochemistry; DNA assay; sensitization; λ-exonuclease; target recycling

INTRODUCTION

Sensitive and selective detection of DNA sequences is significant for genetics therapy, cancer screening, molecular diagnosis, and environmental monitoring, etc.[1-5] Photoelectrochemical (PEC) detection is a recently emerged and vibrantly advancing technique on biological sensing. Due to total separation between detection signal and excitation source, PEC detection has a high sensitivity and low background signal comparing with traditional optical and electrochemical assays.[6,7] Up to now, many different kinds of target analytes such as metal ions, proteins, DNA, microRNA and cells have been successfully detected by PEC assays. Photocurrent output of the

PEC system is a key factor for detection sensitivity of the PEC biosensor, which depends mainly upon the photoactive species utilized in the PEC system. Combining sensitization agents of small band gap photoactive species with wide band gap substrate material to produce sensitization structure with cascade band-edge levels can strengthen light harvest, promote charge separation, and therefore increase the photocurrent output.[8-10] The photoactive materials involved in PEC detection could be divided into two categories, organic and inorganic types. The organic photoactive materials mainly related to dye molecules including ruthenium complexes,[11] porphyin,[12] carboxylated perylene,[13] phthalocyanine,[14] etc, and they possess the features of various electron configuration, wide range absorption, and high light absorption efficiency.[15-17] For another, the inorganic photoactive materials belong primarily to semiconductor nanostructures and quantum dots such as TiO_2,[18] ZnO,[19] CdS,[20] CdSe,[21] Bi_2S_3,[22] CdTe,[23] etc, and they own the merits of big surface area, high extinction coefficient and fast electric carrier mobility.[24-26] As different kinds of photoactive materials possess its specific properties, the inorganic-organic photoactive nanocomposites could integrate the advantages of inorganic materials with organic materials and further enhance the photocurrent output.[27-29] Currently, the PEC biosensor based on inorganic-organic photoactive nanocomposites sensitization for signal amplification has been a newly developing direction.[30]

To accurately detect low levels of DNA sequences, some typical amplification methods have been explored, such as polymerase chain reaction, hybridization chain reaction, rolling circle amplification, and loop-mediated isothermal amplification.[31-34] These signal amplification methods possess high sensitivity, yet, some downsides still remain, including time-consuming process, introduction of auxiliary substances, sophisticated primer design, precise control of temperature cycling. To circumvent these problems, exonuclease has especially exhibited its promising potential applications. Exonuclease is one kind of processively enzyme catalyzing the

hydrolysis of phosphodiester bond to produce oligonucleotides.[35] Lambda-exonuclease (λ-Exo) is one of the important members in exonuclease family that selectively enjoys double-strand DNA with one 5′-phosphorylated end as a substrate and catalyzes stepwise hydrolysis of the 5'-phosphorylated strand in the direction of 5' to 3'.[36] Its nuclease activity is metal-dependent, with a stronger preference for Mg^{2+} ions.[37] λ-Exo assisted target recycling refers to that the sensing electrode was incubated in target solution containing λ-Exo. It not only owns the feature of cycle amplification, but also needs no extra auxiliary substance, no extra incubation time and no labeling step, showing its unique merits.

Herein, we report a novel dual signal amplification strategy by integrating sensitization effect of CdTe/TCPP inorganic-organic nanocomposites with λ-Exo assisted target recycling to develop an enhanced PEC DNA assay, as shown in Scheme 1. The short DNA sequence of Type b3a2, a frequent BCR/ABL fusion gene existing in Chronic Myelogenous Leukemia (CML),[38-40] was selected as target DNA (tDNA). The ZnO nanoplates were firstly coated on an indium tin oxide (ITO) electrode, and calcined with high temperature to form a compact ZnO film. Then, CdS nanocrystals were deposited on the ZnO film by continuous adsorption and reaction between the ions of Cd^{2+} and S^{2-} to form ZnO/CdS hetero-nanostructure. Subsequently, the hairpin DNA (hDNA) was bound on the surface of the CdS nanocrystals firmly via S–Cd bond. Next, in order to block the unbound sites, 6-hydroxy-1-hexanethiol (MCH) was modified on the ITO/ZnO/CdS electrode. When the hDNA modified electrode was incubated with tDNA and λ-Exo, hDNA hybridized with tDNA and changed its conformation from hairpin structure to chainlike double strand. Meanwhile, the λ-Exo assisted tDNA recycling was activated. After the process of tDNA recycling, plenty of short DNA (sDNA) fragments produced on the electrode and hybridize with CdTe/TCPP labeled pDNA (pDNA-CdTe/TCPP conjugates). The photocurrent signal increased dramatically by the sensitization of CdTe/TCPP inorganic-organic nanocomposites coupling with

λ-Exo assisted tDNA recycling. The ingenious PEC DNA assay exhibited a good sensitivity and selectivity for tDNA detection.

<Scheme 1>

EXPERIMENTAL SECTION

Materials of DNA Sequences. The following DNA sequences used were purchased from Sangon Biotech Co., Ltd. (Shanghai, China). Hairpin DNA (hDNA), 5'-phosphorylate-AGA GTT CAA AAG CCC TTC GAG GGA GTG AAG TGTG A GAA GGG CTT TTG TTA GGG-$(CH_2)_6$-SH-3'; probe DNA (pDNA), 5'-HOOC-CCC TAA CAA AAG-3'; target DNA (tDNA), 5'-GAA GGG CTT TTG AAC TCT-3'; one-base mismatch DNA I, 5'-GAA GGG **A**TT TTG AAC TCT-3'; one-base mismatch DNA II, 5'-GAA GGG CTT TTG AA**G** TCT-3'; three-base mismatch DNA, 5'-GAA **C**GG CT**A** TTG AA**G** TCT-3'; noncomplementary DNA, 5'-ACG TGG TCG CCA GCT CTC-3'. Thereinto, the underlined letters in hDNA was the sequences complementary to each other to form the stem of the hDNA.

Other materials as well as apparatus involved in the present work were given in the Supporting Information.

Synthesis of ZnO Nanoplates. ZnO nanoplates were synthesized by hydrothermal reaction with some modifications.[41] Typically, 4 mL of 5 M NaOH was dropwise injected in 21 mL of mixed solution containing $ZnSO_4 \cdot 7H_2O$ (0.75 g) and PEG 20000 (0.75 g), and the solution pH was adjusted to 7.5. After stirred for 1 h at room temperature, the mixed solution was transferred into a 25 mL of Teflon-lined autoclave and heated for 36 h at 120 °C, and then cooled down to the room temperature naturally. The white products were finally acquired by cleaning with deionized (DI) water and then drying for 12 h at 60 °C.

Fabrication of ITO/ZnO/CdS Electrode. Before modification, the bare ITO electrodes were cleaned ultrasonically by acetone, 1 M NaOH of water/ethanol mixture (1:1, v/v), and DI water in order for 20 min of each, and then dried at 100 °C. First, 10 mg of the synthesized ZnO nanoplates were dispersed ultrasonically in 5 mL of DI water, and then 20 μL of this 2.0 mg/mL suspension was scattered onto the ITO electrode with fixed area of 0.25 cm^2. Afterwards, it was naturally dried and then treated at 450 °C for 1 h. The CdS film was modified through continuous ionic layer absorption and reaction method.[24] The ITO/ZnO electrode was alternatively immersed into 0.1 M $Cd(NO_3)_2$ methanol solution and 0.1 M Na_2S methanol/water mixture (1:1, v/v) for 1 min of each and with intermediate methanol washings. After 4 cycles of this dipping produce for CdS nanocrystals deposition, the desired ITO/ZnO/CdS electrode was obtained.

Synthesis of CdTe QDs. Water-soluble, amino-group modified CdTe QDs were synthesized based on the document via utilizing cysteamine as capping agent.[42] Briefly, 6 mmol cysteamine was mixed with 100 mL of 20 mM $CdCl_2$ solution under stirring. The solution pH was then adjusted to 5.8 and deaerated with N_2 for 30 min. Subsequently, 0.10 g $NaBH_4$ and 0.02 g Na_2TeO_3 were successively added into the solution above. The molar ratio of Cd^{2+} / CA / Te^{2-} was 1 / 3 / 0.05. The mixed solution was then heated to 100 °C and refluxed under N_2 protection to obtain the desired CdTe QDs.

Preparation of pDNA-CdTe/TCPP Conjugates. The pDNA and TCPP were simultaneously modified onto the surface of synthesized CdTe QDs through amidation reaction between amino groups on the CdTe QDs and carbonyl groups of the pDNA and TCPP. First, 300 μL of mixed solution consisted of 2 μM pDNA and 1 mM TCPP was activated by 200 μL of 20 mg/mL EDC and NHS solution for 30 min at room temperature to activate carboxyl groups of both pDNA and TCPP. Then, 200 μL of purified solution of CdTe QDs was mixed with the solution above and shaken at 4 °C overnight. After the resulting solution was centrifuged and rinsed with DI water

for some times, the pDNA-CdTe/TCPP conjugates were acquired and dispersed to 1 mL by Tris-HCl buffer (pH=7.4, 10 mM).

Fabrication of DNA Biosensor. Typically, 20 μL of 1 μM hDNA was pretreated by TCEP (10 mM) for 1 h to break disulfide bond and then was dropped on the ITO/ZnO/CdS electrode. After incubated for 12 h at 4 °C, the electrode was washed with Tris-HCl buffer (pH=7.4, 10 mM) and then was covered by 20 μL of 1 mM MCH for 1 h to detach the physically connected hDNA and block the unbound sites. Subsequently, the electrode was incubated with 20 μL of different concentrations of tDNA containing 10 U λ-Exo at 37 °C for 1 h. After washed with Tris-HCl buffer, the electrode was then incubated with 20 μL of fixed concentration of pDNA-CdTe/TCPP conjugates at 37 °C for another 1 h. The resulting electrode was finally introduced into PEC detection after rinsing with Tris-HCl buffer.

PEC measurement. PEC detection was performed at room temperature in Tris-HCl buffer (pH 7.4, 0.1 M) containing 0.1 M ascorbic acid (AA), which served as an efficient electron donor in the course of the PEC test. White light with an irradiation region of 200-2500 nm was utilized as excitation light source and was turned on and off every 10 s. The applied potential was 0.0 V. The AA electrolyte was deaerated by pumping into pure nitrogen for 10 min before the PEC measurement.

RESULTS AND DISCUSSION

Characterization of ZnO Nanoplates. Figure 1A and 1B displays typical powder X-ray diffraction (XRD) pattern and scanning electron microscopy (SEM) image of the synthesized ZnO products, respectively. As exhibited in the XRD pattern, all of the diffraction peaks could be indexed to hexagonal wurtzite structure of ZnO (JCPDS, No. 36-1451). The narrow and sharp diffraction peaks indicated that the obtained ZnO samples had large crystalline domains and a

high degree of crystallinity. It could be observed from the SEM image that the synthesized ZnO samples were plate structures with about 500 nm in length, 15 nm in thickness, and 200 nm in width. The two-dimensional nanoplate structures of the ZnO products could supply large surface area for the deposition of more CdS nanocrystals, which contributed to effective increase in the light absorption and enhancement of the photocurrent intensity.

<Figure 1>

Characterization of CdTe QDs and TCPP. Figure 2A and 2B shows high-resolution transmission electron microscopy (HRTEM) image and UV-visible (UV-vis) absorption spectrum of the synthesized CdTe QDs, respectively. As displayed in Figure 2A, the CdTe QDs had clear lattice fringes and an average size of 3.71 nm could be acquired. The UV-vis absorption spectrum in Figure 2B displayed a broad absorption region to 650 nm with an evident absorption peak at 572 nm, indicating the CdTe QDs could absorb long-wavelength light effectively. Parts A and B of Figure S1 show molecular structure and UV-vis absorption spectrum of the TCPP, respectively. One TCPP molecule has four carboxyl groups, which could covalently bound with CdTe QDs to form stable CdTe/TCPP nanocomposites (Figure S1-A). The absorption spectrum of TCPP includes a strong Soret band at 415 nm as well as some moderate Q-bands at 513, 547, 588, and 655 nm (Figure S1-B).[43] Additionally, the characterization on pDNA-CdTe/TCPP conjugates was shown in Figure S2.

<Figure 2>

Photocurrent Signal Enhanced Mechanism. The sensitivity of the PEC DNA biosensor depended on changing degree of the photocurrent signal when tDNA was detected. The TiO_2/CdS hetero-nanostructure was employed as the substrate photoactive material, whereas the sensitization effect of the CdTe/TCPP inorganic-organic nanocomposites was applied for signal amplification. The transfer mechanism of photogenerated electrons is illustrated in Scheme 2.

ZnO is a large energy gap semiconductor (~3.2 eV) and it can harvest only the ultraviolet light (<420 nm).[44] CdS owns a smaller energy band gap of 2.4 eV and it extends the absorption to middle-wavelength light (<550 nm).[45] In addition, CdS has a higher edge of conduction band (CB) comparing with ZnO, which is beneficial to inflow of excited electrons from CdS to ZnO.[46] Therefore, the TiO_2/CdS hetero-nanostructure could inhibit the electron-hole recombination and increase photocurrent output effectively. The sensitization of CdTe/TCPP nanocomposites could play the advantages of both inorganic and organic photoactive materials and evidently promote the photocurrent signal. As a popular inorganic sensitization agent, CdTe QDs own a small energy band gap (~1.4 eV) and it can reach the absorption to long wavelength light (~650 nm, shown as Figure 2B). Porphyrin is one kind of organic photosensitizers often used in dye sensitized solar cells because of its very strong absorption in the region of 400-450 nm (Soret band) and the normal absorption in the zone of 500-700 nm (Q-bands).[47] As a member among the porphyrin family, TCPP owns a energy band gap of 2.5 eV,[48] and its absorption mainly located at the region of middle-wavelength light (as shown in panel B of Figure S1). Due to large surface area of the CdTe QDs, plenty of TCPP molecules could be covalently linked to form CdTe/TCPP inorganic-organic nanocomposites. CdTe QDs effectively enlarged the absorption range of the PEC system, whereas TCPP molecules evidently strengthened the absorption intensity of the PEC system. Accordingly, the sensitization of the CdTe/TCPP nanocomposites could promote the photocurrent signal notably.

The enzyme of λ-Exo could assist tDNA recycle to further enhance the sensitization effect of the CdTe/TCPP nanocomposites. In the existence of tDNA, the hDNA hybridized with tDNA and changed its conformation from hairpin structure to chainlike double strand. At this time, the hybridized hDNA would be cleaved specifically by λ-Exo to set free tDNA. The λ-Exo has no activity on non-hybridized hDNA, because the 5'-phosphorylated end of the hDNA has 6-bases

overhang.[35] The rest of non-hybridized hDNA on the electrode continuously hybridized with the released tDNA to form chainlike DNA duplex, which could be further cleaved by λ-Exo and set free tDNA again. After multiple times for tDNA recycling, more amounts of sDNA fragments coming from digestion of hDNA was produced on the sensing electrode and hybridized with the pDNA-CdTe/TCPP conjugates. Thus, the photocurrent signal dramatically increased by the sensitization effect of the CdTe/TCPP inorganic-organic nanocomposites coupling with λ-Exo assisted tDNA recycling.

<Scheme 2>

EIS Characterization of the DNA Biosensor. Electrochemical impedance spectroscopy (EIS) is a facile and useful technique for monitoring the features of the modified electrodes by probing the interface properties. Figure 3A shows impedance spectra for different build steps of the DNA biosensor, and each impedance spectrum consisted of a semicircle at higher frequencies and a linear part at lower frequencies. The semicircle presented the limited process for electron-transfer, whereas the linear part revealed the diffusion-limited process. The diameter of the semicircle, which reflected the restricted diffusion of the redox probe accessing the electrode interface, equaled the electron-transfer resistance (R_{et}). For ITO/ZnO electrode, the impedance spectrum showed a small semicircle (curve a), implying a relatively small R_{et} value. After the modification of CdS nanocrystals, the R_{et} increased due to low conductivity of semiconductors (curve b). With the immobilization of hDNA and MCH, the R_{et} increased evidently (curve c). It was because that (i) both hDNA sequences and MCH molecules had low conductivities; (ii) phosphate groups of hDNA produced a negatively charged layer that reduced the ability of $[Fe(CN)_6]^{3-/4-}$ redox probe approaching the electrode interface. Once the electrode was incubated with tDNA and λ-Exo, the R_{et} decreased obviously (curve d), indicating that the DNA duplex structure was successfully cleaved by λ-Exo and a large number of sDNA fragments were produced on the electrode

surface. While the electrode was further incubated with pDNA-CdTe/TCPP conjugates, the R_{et} increased again (curve e), which was ascribed to lower electron-transfer abilities of the DNA sequences, CdTe QDs and TCPP molecules. The expectably changed R_{et} suggested successful fabrication of the proposed DNA biosensor.

<Figure 3>

PEC Characterization of the DNA Biosensor. The build procedure of the DNA biosensor was further characterized by photocurrent response, as displayed in Figure 3B. The ITO/ZnO electrode showed a low photocurrent intensity (curve a, I=4.03 μA), because ZnO has a large band gap and it can absorb only the ultraviolet light, causing a low photocurrent output. After modification of CdS nanocrystals, the photocurrent intensity obviously strengthened (curve b, I=24.47 μA). It was mainly because that the ZnO nanoplates with large surface area could carry plenty of CdS nanocrystals and the formation of the ZnO/CdS hetero-nanostructure extended the light absorption range. The photocurrent intensity decreased after immobilization of hDNA and MCH (curve c, I=15.25 μA), which could be explained by weak charge-transfer abilities of both hDNA sequences and MCH molecules. While the electrode was then incubated with tDNA and λ-Exo, the photocurrent intensity increased moderately (curve d, I=19.72 μA). It was because that the formed DNA duplex structure could be cleaved by λ-Exo and the produced sDNA fragments had better charge-transfer ability than hDNA. After pDNA-CdTe/TCPP conjugates were bound on the electrode via DNA hybridization between pDNA and sDNA, the photocurrent intensity increased significantly (curve e, I=43.06 μA). It could be attributed to high-efficient sensitization of the CdTe/TCPP inorganic-organic nanocomposites. Besides, CdTe QDs were also used as sensitization agents instead of CdTe/TCPP nanocomposites to carry out the control experiment. The comparison results showed that the photocurrent increment to CdTe QDs was only 56.8% of that to CdTe/TCPP nanocomposites, confirming superiority of the CdTe/TCPP inorganic-organic

photoactive nanocomposites as signal amplifiers. Accordingly, the PEC characterization proved successful fabrication of the DNA biosensor.

Optimal Conditions of the DNA Biosensor. Figure S3-A shows photocurrent intensity of the ITO/ZnO electrode fabricated with different concentrations of ZnO nanoplates suspension. Elevating the suspension concentration at first could modify more ZnO nanoplates on the ITO electrode. As a result, the ITO/ZnO electrode adsorbed more light and the photocurrent intensity increased. When the suspension concentration of the ZnO nanoplates reached 2.0 mg/mL, the fabricated ITO/ZnO electrode owned the maximum photocurrent intensity. With further elevating the suspension concentration, a growing number of surface recombination sites formed on the excess ZnO nanoplates and the diffusion resistance for the ZnO film raised, causing gradual decrease in the photocurrent intensity.[49] Thus, 2.0 mg/mL suspension concentration of the ZnO nanoplates was used for fabricating the electrode.

Figure S3-B exhibits photocurrent intensity of the ITO/ZnO/CdS electrode fabricated with different cycles of CdS nanocrystals. Initially, along with the cycle number increased, the deposition of CdS nanocrystals gradually raised, resulting in more light absorption and increased photocurrent. However, with further increase in cycle number, the photocurrent intensity gradually decreased, because the excessive amount of CdS nanocrystals acted as surface recombination centers, which evidently enlarged the diffusion resistance for electron motion. It could be observed that the ITO/ZnO/CdS electrode deposited with 6 cycles of CdS reached the maximum photocurrent value. Yet, as the absorption band of the deposited CdS nanocrystals reached 550 nm, which partly overlapped with that of the two layers of subsequently labeled CdTe QDs and TCPP molecules. For the purpose of acquiring optimal signal amplification, 4 deposition cycles of CdS nanocrystals was chosen for fabricating the DNA biosensor.

The enzyme of λ-Exo could cleave the hybridized hDNA to release the tDNA for recycling. Hence, the incubation time of the sensing electrode in λ-Exo involved solution had a significant influence on the photocurrent signal. Figure S3-C shows photocurrent responses of the DNA biosensor for different incubation times in 20 μL of 1 μM tDNA containing 10 U λ-Exo. It could be seen that the photocurrent intensity gradually enhanced with extension of the incubation time and came to a plateau at 60 min afterwards, indicating the achievement of tDNA recycling assisted by λ-Exo. Hence, the optimal incubation time 60 min was selected.

PEC Detection of tDNA. Based upon dual signal amplification via coupling inorganic-organic nanocomposites sensitization with λ-Exo assisted target recycling, the tDNA could be detected selectively and sensitively by this PEC DNA assay. Figure 4A shows the photocurrent signals of the PEC DNA biosensor to tDNA solution with varied concentrations. The photocurrent signal augmented gradually by elevating the concentration of tDNA from 0 to 1.0 nM. As displayed in Figure 4B, the photocurrent signals presented a nice linear relation to logarithm of tDNA concentration in the scope of 0.1 fM to 5 pM. The equation of linear regression was $I = 23.24 + 4.40 \log C$ (fM), with the correlation of 0.9971. The lowest detection limit was calculated to be 25.6 aM at the signal-to-noise ratio of 3. The sensitivity of this PEC DNA assay was compared with previously reported PEC assays as well as other analytical protocols. The comparison results were displayed in Table S1, and it demonstrated that the dual signal amplification strategy indeed offered a much better detection limit and a wider linear response scope. Moreover, to illustrate synergistic effect about this tactics for dual signal amplification, detection performance of the PEC DNA biosensor just without λ-Exo incubation was investigated (Figure S4). The PEC detection results presented that the latter DNA biosensor offered a linear detection scope of 1 fM to 100 pM and a calculated detection limit of 0.32 fM. It could be obtained that the sensitivity of the DNA biosensor with λ-Exo incubation was about 12 times better than that without λ-Exo

incubation. Thus, this control experiment also pointed an obvious superiority for the designed dual signal amplification tactics.

<Figure 4>

Selectivity, Reproducibility and Stability of the DNA Assay. The selectivity of the PEC DNA assay was evaluated via making a comparison of the photocurrent responses to diverse DNA sequences involving tDNA, one-base mismatch DNA at different locations, three-base mismatch DNA, and noncomplementary DNA under the equal concentration (10 fM). As presented in Figure 5, the photocurrent response to tDNA displayed an evident increase than that of the blank solution. The photocurrent increases to one-base mismatch DNA at different locations were also observed, however, they could be almost ignored compared with the tDNA detection. Additionally, the photocurrent responses to noncomplementary DNA and three-base mismatch DNA were very close to the blank solution. All these comparison results pointed the photocurrent signal was triggered specifically via the hybridization between tDNA and hDNA, and further amplified by inorganic-organic nanocomposites sensitization as well as λ-Exo assisted target recycling. It was demonstrated that the designed PEC DNA assay had a satisfied selectivity.

<Figure 5>

The reproducibility of the proposed DNA assay was estimated with inter-assay relative standard deviation (RSD) of five sensing electrodes prepared independently. After the hDNA modified sensing electrodes were first incubated in 20 μL of different concentrations of tDNA containing 10 U λ-Exo and then further incubated with pDNA-CdTe/TCPP conjugates, the photocurrent responses gave out the RSDs of 3.5%, 3.9% and 3.6% corresponding to 1.0 fM, 10 fM and 100 fM tDNA detection (Table S2), which indicated an acceptable reproducibility and accuracy of this DNA assay.

The stability of the PEC DNA assay was assessed via testing the photocurrent change of the sensing electrode. Two groups of hDNA modified sensing electrodes were first fabricated in the identical situations and each group consisted of five electrodes. The photocurrent intensities for the first group electrodes were tested without storage time, and the average photocurrent response was used as the original value of the sensing electrode. After being stored in a humid condition at 4 °C for a month, the average photocurrent response of the second group electrodes remained at 96.1% of its original value, implying good storage stability.

CONCLUSIONS

In summary, a novel enhanced PEC DNA assay was established by coupling inorganic-organic nanocomposites sensitization with λ-Exo assisted target recycling for dual signal amplification. The sensitization effect of CdTe/TCPP nanocomposites could take the advantages of both inorganic and organic photoactive materials, and accordingly increase the photocurrent intensity evidently. The enzyme of λ-Exo could assist tDNA recycling to further promote the sensitization of the CdTe/TCPP nanocomposites. The well-designed PEC DNA assay offered a low detection limit with a wide detection scope for target DNA detection. Also, the proposed DNA assay can be widely applied to detect various DNA sequences, especially to those short specific DNA sequences. On account of its high sensitivity and good selectivity, this signal amplification strategy may open a new prospect to detect trace levels of DNA sequences and offer an effective evaluation to early diagnosis of various diseases.

AUTHOR INFORMATION

Corresponding Authors

*E-mail: iamqmshen@njupt.edu.cn; jjzhu@nju.edu.cn.

Author Contributions

[1] X.M.S. and G.C.F. contributed equally to this work.

ACKNOWLEDGMENTS

We appreciate the financial support by the National Natural Science Foundation of China (21575069, 21603099 and 21335004), Foundation of the Jiangsu Education Committee (14KJB150015), Synergetic Innovation Center for Organic Electronics and Information Displays, and Ministry of Education of China (No. IRT1148).

ASSOCIATED CONTENT

Supporting Information

The Supporting Information:

Materials, apparatus, characterization of TCPP (Figure S1), characterization of pDNA-CdTe/TCPP conjugates (Figure S2), optimization of experimental conditions (Figure S3), comparison of various methods for tDNA detection (Table S1), detection performance of the DNA biosnesor without λ-Exo (Figure S4), and photocurrent responses of the DNA biosensor for reproducibility test (Table S2).

REFERENCES

(1) Maddocks, O. D. K.; Labuschagne, C. F.; Adams, P. D.; Vousden, K. H. Serine Metabolism Supports the Methionine Cycle and DNA/RNA Methylation through De Novo ATP Synthesis in Cancer Cells. *Molecular Cell* **2016**, *61*, 210–221.

(2) Meng, H. M.; Liu, H.; Kuai, H. L.; Peng, R. Z.; Mo, L. T.; Zhang, X. B. Aptamer-integrated DNA Nanostructures for Biosensing, Bioimaging and Cancer Therapy. *Chem. Soc. Rev*. **2016**, *45*, 2583–2602.

(3) Huang, Y.; Zhang, Y. L.; Xu, X. M.; Jiang, J. H.; Shen, G. L.; Yu, R. Q. Highly Specific and Sensitive Electrochemical Genotyping via Gap Ligation Reaction and Surface Hybridization Detection. *J. Am. Chem. Soc.* **2009**, *131*, 2478–2480.

(4) Mozaz, S. R.; Alda, M. J. L.; Barceló, D. Biosensors as Useful Tools for Environmental Analysis and Monitoring. *Anal. Bioanal. Chem*. **2006**, *386*, 1025–1041.

(5) Huang, J.; Wu, Y. R.; Chen, Y.; Zhu, Z.; Yang, X. H.; James Yang, C. Y.; Wang, K. M.; Tan, W. H. Pyrene-excimer Probes Based on the Hybridization Chain Reaction for the Detection of Nucleic Acids in Complex Biological Fluids. *Angew. Chem. Int. Ed.* **2011**, *50*, 401−404.

(6) Zhao, W. W.; Xu, J. J.; Chen, H. Y. Photoelectrochemical DNA Biosensors. *Chem. Rev.* **2014**, *114*, 7421−7441.

(7) Zhao, W. W.; Xu, J. J.; Chen, H. Y. Photoelectrochemical Bioanalysis: The State of the Art. *Chem. Soc. Rev.* **2015**, *44*, 729−741.

(8) Fan, G. C.; Ren, X. L.; Zhu, C.; Zhang, J. R.; Zhu, J. J. A New Signal Amplification Strategy of Photoelectrochemical Immunoassay for Highly Sensitive Interleukin-6 Detection Based on TiO_2/CdS/CdSe Dual Co-sensitized Structure. *Biosens. Bioelectron.* **2014**, *59*, 45–53.

(9) Lee, Y. L.; Lo, Y. S. Highly Efficient Quantum-dot-sensitized Solar Cell Based on Co-sensitization of CdS/CdSe. *Adv. Funct. Mater.* **2009**, *19*, 604–609.

(10) Santra, P. K.; Kamat, P. V. Mn-doped Quantum Dot Sensitized Solar Cells: A Strategy to Boost Efficiency over 5%. *J. Am. Chem. Soc.* **2012**, *134*, 2508−2511.

(11) Zhang, X. R.; Xu, Y. P.; Zhao, Y. Q.; Song, W. L. A New Photoelectrochemical Biosensor Based on DNA Conformational Changes and Isothermal Circular Strand-displacement Polymerization Reaction. *Biosens. Bioelectron.* **2013**, *39*, 338–341.

(12) Hu, Y. Q.; Xue, Z. H.; He, H. X.; Ai, R. X.; Liu, X. H.; Lu, X. Q. Photoelectrochemical Sensing for Hydroquinone Based on Porphyrin-functionalized Au Nanoparticles on Graphene. *Biosens. Bioelectron.* **2013**, *47*, 45–49.

(13) Lou, J.; Liu, S. S.; Tu, W. W.; Dai, Z. H. Graphene Quantum Dots Combined with Endonuclease Cleavage and Bidentate Chelation for Highly Sensitive Electrochemiluminescent DNA Biosensing. *Anal. Chem.* **2015**, *87*, 1145−1151.

(14) Li, H. B.; Xue, Y.; Wang, W. Femtomole Level Photoelectrochemical Aptasensing for Mercury Ions Using Quercetin-copper (II) Complex as the DNA Intercalator. *Biosens. Bioelectron.* **2014**, *54*, 317–322.

(15) Peumans, P.; Yakimov, A.; Forrest, S. R. Small Molecular Weight Organic Thin-film Photodetectors and Solar Cells. *J. Appl. Phys.* **2003**, *93*, 3693–3722.

(16) Kim, S.; Lee, J. K.; Kang, S. O.; Ko, J.; Yum, J. H.; Fantacci, S.; Angelis, F. D.; Censo, D. D.; Nazeeruddin, M. K.; Gratzel, M. Molecular Engineering of Organic Sensitizers for Solar Cell Applications. *J. Am. Chem. Soc.* **2006**, *128*, 16701–16707.

(17) Ameri, T.; Dennler, G.; Lungenschmied, C.; Brabec, C. J. Organic Tandem Solar Cells: A Review. *Energy Environ. Sci.* **2009**, *2*, 347–363.

(18) Lu, W.; Jin, Y.; Wang, G.; Chen, D.; Li, J. Enhanced Photoelectrochemical Method for Linear DNA Hybridization Detection Using Au-nanopaticle Labeled DNA as Probe onto Titanium Dioxide Electrode. *Biosens. Bioelectron.* **2008**, *23*, 1534–1539.

(19) Tu, W. W.; Lei, J. P.; Wang, P.; Ju, H. X. Photoelectrochemistry of Free-base-porphyrin-functionalized Zinc Oxide Nanoparticles and Their Applications in Biosensing. *Chem. Eur. J.* **2011**, *17*, 9440–9447.

(20) Zhao, W. W.; Yu, P. P.; Shan, Y.; Wang, J.; Xu, J. J.; Chen, H. Y. Exciton-plasmon Interactions Between CdS Quantum Dots and Ag Nanoparticles in Photoelectrochemical System and Its Biosensing Application. *Anal. Chem.* **2012**, *84*, 5892−5897.

(21) Zhang, X. R.; Li, S. G.; Jin, X.; Li, X. M. Aptamer Based Photoelectrochemical Cytosensor with Layer-by-layer Assembly of CdSe Semiconductor Nanoparticles as Photoelectrochemically Active Species. *Biosens. Bioelectron.* **2011**, *26*, 3674−3678.

(22) Yin, H. S.; Sun, B.; Zhou, Y. L.; Wang, M.; Xu, Z. N.; Fu, Z. L.; Ai, S. Y. A New Strategy for Methylated DNA Detection Based on Photoelectrochemical Immunosensor Using Bi_2S_3 Nanorods, Methyl Bonding Domain Protein and Anti-his Tag Antibody. *Biosens. Bioelectron.* **2014**, *51*, 103−108.

(23) Fan, G. C.; Han, L.; Zhu, H.; Zhang, J. R.; Zhu, J. J. Ultrasensitive Photoelectrochemical Immunoassay for Matrix Metalloproteinase-2 Detection Based on CdS:Mn/CdTe Cosensitized TiO_2 Nanotubes and Signal Amplification of SiO_2@Ab_2 Conjugates. *Anal. Chem.* **2014**, *86*, 12398–12405.

(24) Li, T. L.; Lee, Y. L.; Teng, H. S. High-performance Quantum Dot-sensitized Solar Cells Based on Sensitization with $CuInS_2$ Quantum Dots/CdS Heterostructure. *Energy Environ. Sci.* **2012**, *5*, 5315–5324.

(25) Tisdale, W. A.; Williams, K. J.; Timp, B. A.; Norris, D. J.; Aydil, E. S.; Zhu, X. Y. Hot-electron Transfer from Semiconductor Nanocrystals. *Science.* **2010**, *328*, 1543–1547.

(26) Beard, M. C. Multiple Exciton Generation in Semiconductor Quantum Dots. *J. Phys. Chem. Lett.* **2011**, *2*, 1282–1288.

(27) Choi, H.; Nicolaescu, R.; Paek, S.; Ko, J.; Kamat, P. V. Supersensitization of CdS Quantum Dots with a Near-infrared Organic Dye: Toward the Design of Panchromatic Hybrid-sensitized Solar Cells. *ACS Nano* **2011**, *5*, 9238–9245.

(28) Lelii, C.; Bawendi, M. G.; Biagini, P.; Chen, P. Y.; Crucianelli, M.; Darcy, J. M.; Angelis, F. D.; Hammond, P. T.; Po, R. Enhanced Photovoltaic Performance with Co-sensitization of Quantum Dots and an Organic Dye in Dye-sensitized Solar Cells. *J. Mater. Chem. A*. **2014**, *2*, 18375–18382.

(29) Meng, K.; Surolia, P. K.; Byrne, O.; Thampi, R. Quantum Dot and Quantum Dot-dye Co-sensitized Solar Cells Containing Organic Thiolateedisulfide Redox Electrolyte. *J. Power Sources* **2015**, *275*, 681–687.

(30) Fan, G. C.; Zhao, M.; Zhu, H.; Shi, J. J.; Zhang, J. R.; Zhu, J. J. Signal-on Photoelectrochemical Aptasensor for Adenosine Triphosphate Detection Based on Sensitization Effect of CdS:Mn@$Ru(bpy)_2$(dcbpy) Nanocomposites. *J. Phys. Chem. C* **2016**, *120*, 15657–15666.

(31) Mahmoudian, L.; Kaji, N.; Tokeshi, M.; Nilsson, M.; Baba, Y. Rolling Circle Amplification and Circle-to-circle Amplification of a Specific Gene Integrated with Electrophoretic Analysis on a Single Chip. *Anal. Chem.* **2008**, *80*, 2483–2490.

(32) Chen, Y.; Xu, J.; Su, J.; Xiang, Y.; Yuan, R.; Chai Y. In Situ Hybridization Chain Reaction Amplification for Universal and Highly Sensitive Electrochemiluminescent Detection of DNA. *Anal. Chem.* **2012**, *84*, 7750−7755.

(33) Li, H.; Huang, J.; Lv, J.; An, H.; Zhang, X. Zhang, Z.; Fan, C.; Hu, J. Nanoparticle PCR: Nanogold-assisted PCR with Enhanced Specificity. *Angew. Chem. Int. Ed.* **2005**, *44*, 5100–5103.

(34) Li, C. P.; Li, Z. P.; Jia, H. X.; Yan, J. L. One-step Ultrasensitive Detection of microRNAs with Loop-mediated Isothermal Amplification (LAMP). *Chem. Commun.* **2011**, *47*, 2595–2597.

(35) Mitsis, P. G.; Kwagh, J. G. Characterization of the Interaction of Lambda Exonuclease with the Ends of DNA. *Nucleic Acids Res.* **1999**, *27*, 3057–3063.

(36) Kovall, R.; Matthews, B. W. Toroidal Structure of λ-Exonuclease. *Science* **1997**, *277*, 1824–1827.

(37) Little, J. W.; Lehman, I. R.; Kaiser, A. D. An Exonuclease Induced by Bacteriophage λ. *J. Biol. Chem.* **1967**, *242*, 672–678.

(38) Kantarjian, H. M.; Deisseroth, A.; Kurzrock, R.; Estrov, Z.; Talpaz, M. Chronic Myelogenous Leukemia: A Concise Update. *Blood* **1993**, *82*, 691–703.

(39) Yoo, S. J.; Seo, E. J.; Lee, J. H.; Seo, Y. H.; Park, P. W.; Ahn, J. Y. A Complex, Four-way Variant t(15;17) in Acute Promyelocytic Leukemia. *Cancer Genet. Cytogenet.* **2006**, *167*, 168–171.

(40) Lin, X. H.; Wu, P.; Chen, Wei.; Zhang, Y. F.; Xia, X. H. Electrochemical DNA Biosensor for the Detection of Short DNA Species of Chronic Myelogenous Leukemia by Using Methylene Blue. *Talanta* **2007**, *72*, 468–471.

(41) Shang, T. M.; Sun, J. H.; Zhou, Q. F.; Guan, M. Y. Controlled Synthesis of Various Morphologies of Nanostructured Zinc Oxide: Flower, Nanoplate, and Urchin. *Cryst. Res. Technol.* **2007**, *42*, 1002−1006.

(42) Fan, G. C.; Han, L.; Zhang, J. R.; Zhu, J. J. Enhanced Photoelectrochemical Strategy for Ultrasensitive DNA Detection Based on Two Different Sizes of CdTe Quantum Dots Cosensitized TiO_2/CdS:Mn Hybrid Structure. *Anal. Chem.* **2014**, *86*, 10877−10884.

(43) Bera, R.; Mandal, S.; Mondal, B.; Jana, B.; Nayak, S. K.; Patra, A. Graphene-porphyrin Nanorod Composites for Solar Light Harvesting. *ACS Sustainable Chem. Eng.* **2016**, *4*, 1562−1568.

(44) Wang, X. D.; Gao, P. X.; Li, J.; Summers, C. J.; Wang, Z. L. Rectangular Porous ZnO-ZnS Nanocables and ZnS Nanotubes. *Adv. Mater.* **2002**, *14*, 1732−1735.

(45) Lee, Y. L.; Chi, C. F.; Liau, S. Y. CdS/CdSe Co-sensitized TiO_2 Photoelectrode for Efficient Hydrogen Generation in a Photoelectrochemical Cell. *Chem. Mater.* **2010**, *22*, 922−927.

(46) Li, C.; Yang, L.; Xiao, J.; Wu, Y. C.; Søndergaard M.; Luo, Y.; Li, D.; Meng, Q.; Iversen B. B. ZnO Nanoparticle Based Highly Efficient CdS/CdSe Quantum Dot-sensitized Solar Cells. *Phys. Chem. Chem. Phys.* **2013**, *15*, 8710−8715.

(47) Cherian, S.; Wamser, C. C. Adsorption and Photoactivity of Tetra(4-carboxyphenyl)-porphyrin (TCPP) on Nanoparticulate TiO_2. *J. Phys. Chem. B* **2000**, *104*, 3624−3629.

(48) Liu, J.; Gu, P.; Zhou, F.; Xu, Q.; Lu, J.; Li, H.; Wang, L. Preparation of TCPP: Block Copolymer Composites and Study of Their Memory Behavior by Tuning the Loading Ratio of TCPP in the Polymer Matrix. *J. Mater. Chem. C* **2013**, *1*, 3947–3954.

(49) Anta, J. A.; Guillen, E.; Tena-Zaera, R. ZnO-based Dye-sensitized Solar Cells. *J. Phys. Chem. C* **2012**, *116*, 11413−11425.

Figures

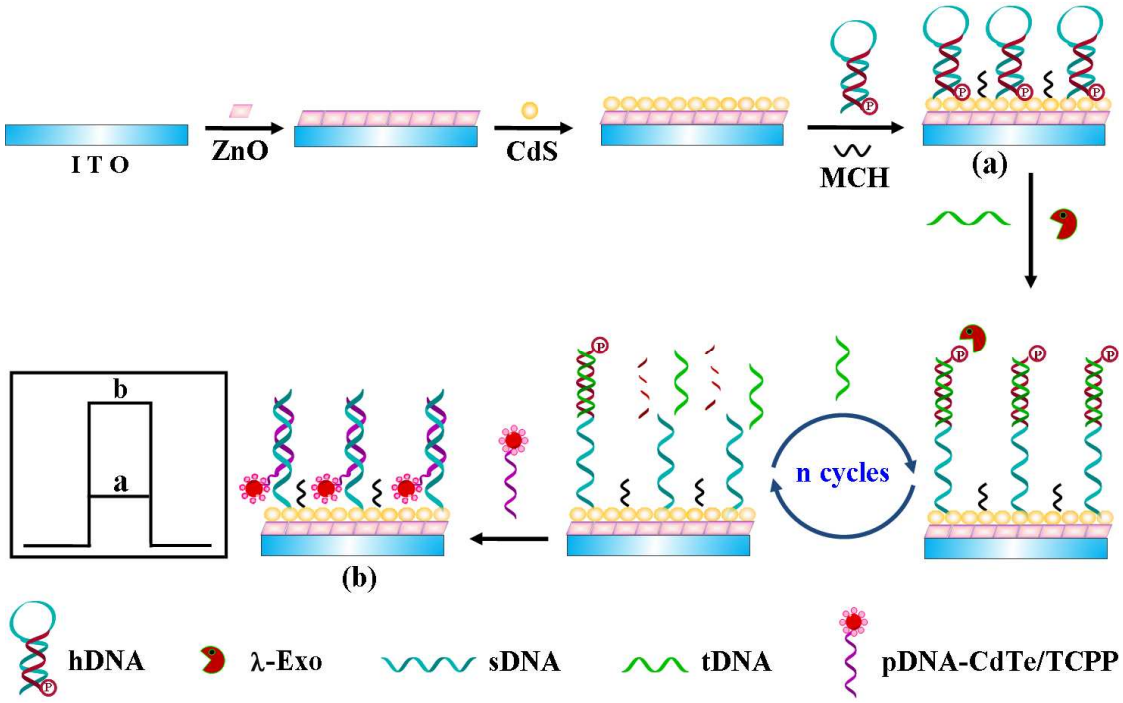

Scheme 1. Build produce of the designed PEC DNA biosensor.

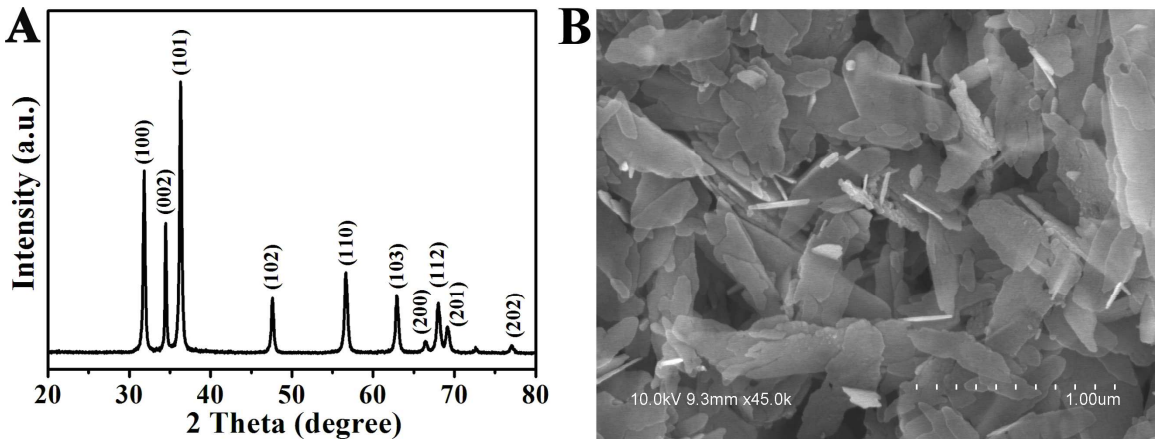

Figure 1. (A) Powder XRD pattern and (B) SEM image of the synthesized ZnO nanoplates.

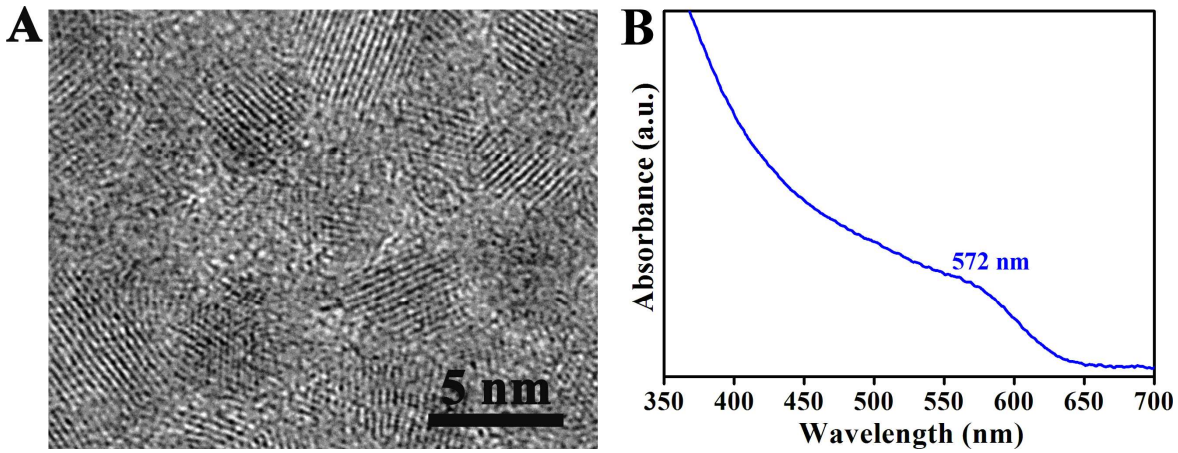

Figure 2. (A) HRTEM image and (B) UV-vis absorption spectrum of the obtained CdTe QDs.

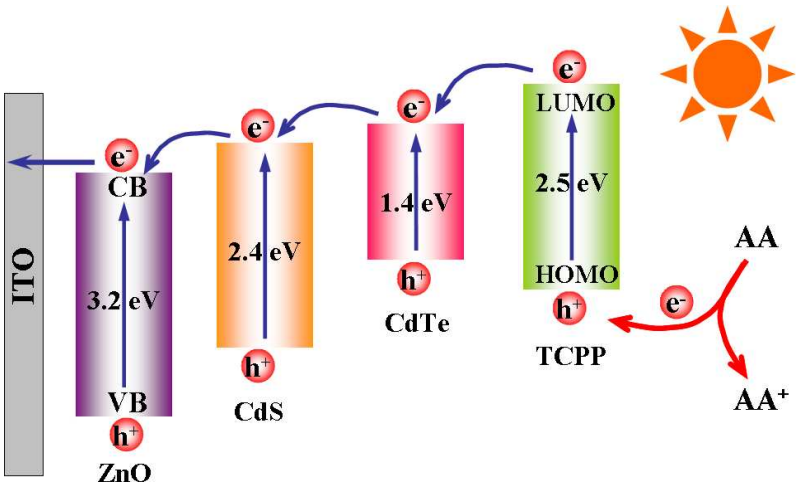

Scheme 2. Transfer mechanism of the photogenerated electrons in the PEC DNA biosensor.

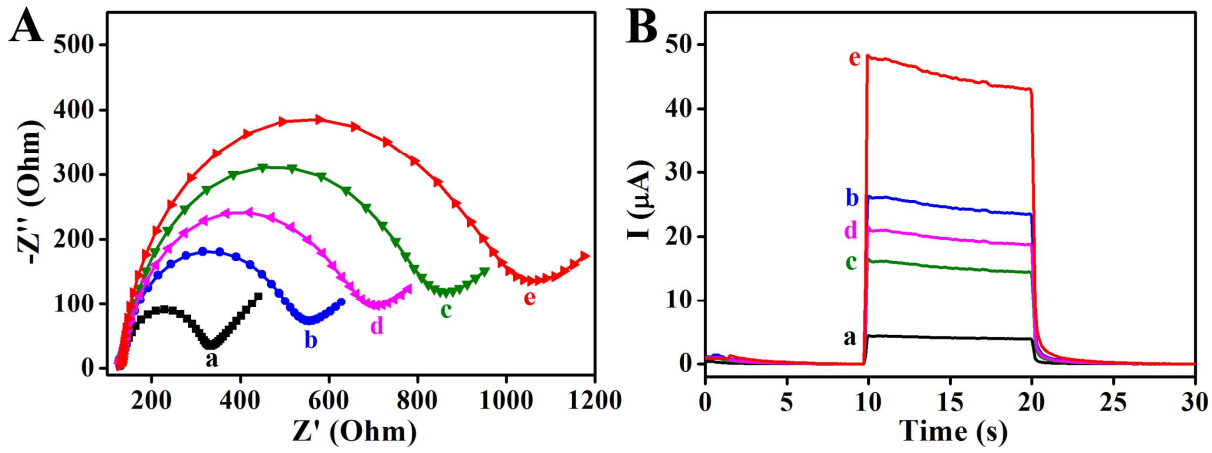

Figure 3. (A) EIS and (B) photocurrent responses of (a) the ITO/ZnO electrode, (b) after CdS nanocrystals modification, (c) after hDNA and MCH immobilization, (d) after incubated with 20 μL of 1 μM tDNA containing 10 U λ-Exo, and (e) after further incubated with 20 μL of fixed concentration of pDNA-CdTe/TCPP conjugates.

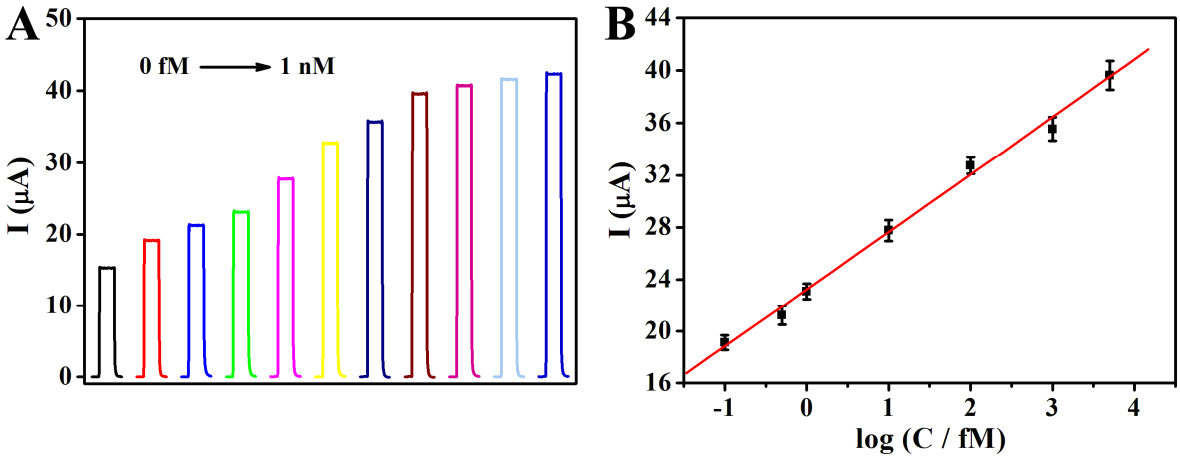

Figure 4. (A) Photocurrent responses of the PEC DNA biosensor to different concentrations of tDNA (0, 0.1, 0.5, 1.0, 10, 100 fM, 1, 5, 10 and 100 pM, and 1.0 nM); (B) Calibration curve of the PEC DNA biosensor to tDNA solution with varied concentrations. The error bars display standard deviations of five parallel tests.

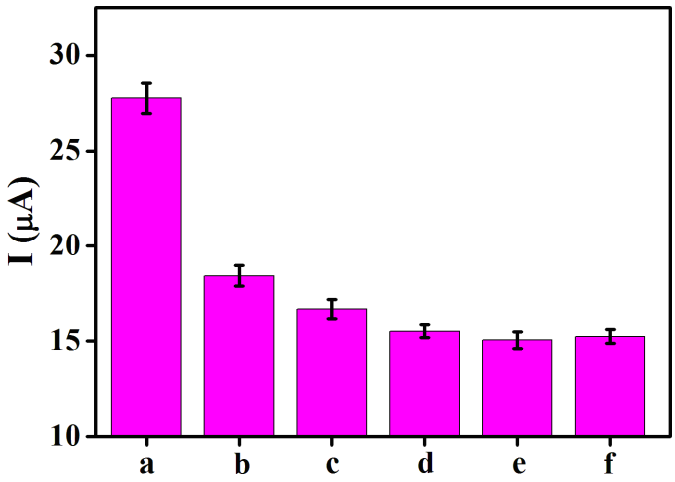

Figure 5. Photocurrent responses of the PEC DNA biosensor to 20 μL of 10 fM different DNA sequences: (a) tDNA, (b) one-base mismatch DNA I, (c) one-base mismatch DNA II, (d) three-base mismatch DNA, (e) noncomplementary DNA, and (f) blank. The error bars present standard deviations of five replicated determinations.

For TOC only

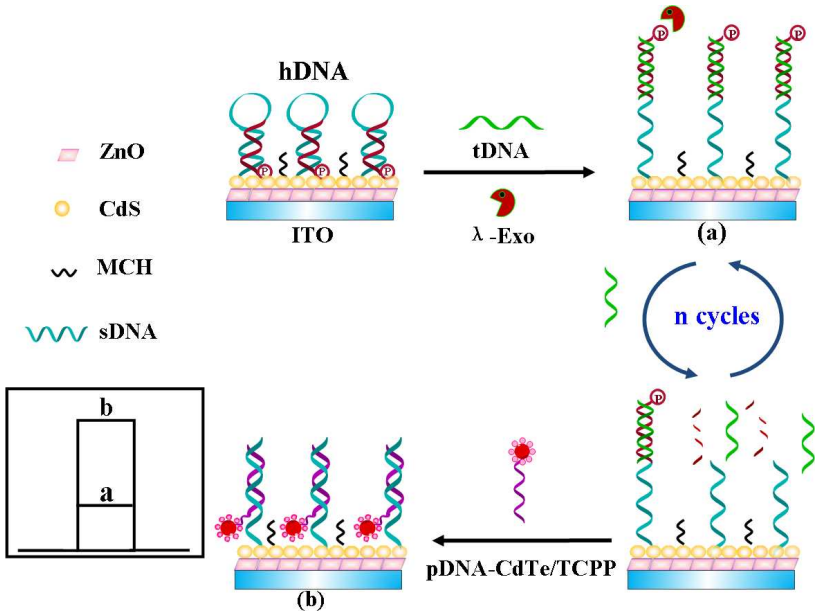
hDNA
ZnO
CdS
MCH
sDNA
ITO
tDNA
λ -Exo
(a)
n cycles
b
a
pDNA-CdTe/TCPP
(b)